ALTERNATE MECHANISMS FOR SPIN POLARIZATION

Bastiaan Driehuys, Ph.D.
Duke University, Department of Radiology, Durham, NC 27710

1. INTRODUCTION

Since the introduction of hyperpolarized ^{129}Xe MR imaging [1] there has been a relative explosion of novel polarization methods and a rediscovery of older polarization methods. The term "hyperpolarized" refers to a nuclear spin ensemble whose polarization is higher than could be achieved by letting spins relax to thermal equilibrium in the imaging magnet. Thermal polarization is typically around ~10^{-6}, whereas hyperpolarization can approach 1. Hyperpolarization, thus potentially provides 6 orders of magnitude in SNR increase for an MRI experiment. The pantheon of nuclei which have been hyperpolarized and imaged now include ^{1}H, ^{3}He, ^{13}C, ^{15}N, and ^{129}Xe. The aim of this course is to present a review of hyperpolarization methods, current performance levels, and areas of application.

2. SIGNAL AND POLARIZATION

The relationship between polarization and NMR signal is worth working through from basics without the usual assumptions of thermal equilibrium. To observe an MR signal there must be an imbalance of spins pointing along the field versus against the field. Otherwise the oppositely phased signals from the two spin states cancel each other in the transverse plane. The size of the MR signal is also proportional to the nuclear magnetic moment μ, or gyromagnetic ratio γ, which is related via $\mu=\hbar\gamma I$, where I is the nuclear spin. The voltage induced in the receiver coil can be simply derived from Faraday's Law

$$V_{signal} = G_{coil}\,\gamma\,\omega\left(N_{+} - N_{-}\right) \qquad [1]$$

where G_{coil} is a coil sensitivity factor, and N_+ and N_- are number of spins aligned and anti-aligned with the magnetic field. It is convenient to define polarization P as

$$P = \frac{N_{+} - N_{-}}{N_{+} + N_{-}} \qquad [2]$$

The induced signal voltage in terms of polarization is then

$$V_{signal} = G_{coil}\,\gamma\,\omega_0\,N\,P \qquad [3]$$

The key message, as we already suspected, is that MR signal scales linearly with polarization.

2.1 Thermal Polarization Basics

We should briefly understand thermal polarization in order to fully appreciate hyperpolarization. Thermal polarization is created because it is slightly more energetically favorable for nuclear moments to align with the magnetic field than against it. The interaction energy of a dipole with a magnetic field is $\mu \cdot B$ and for a spin ½ system creates a low and high energy states of energy $-\mu B$ and μB. Boltzmann statistics teach us to calculate the relative spin populations via the partition function

$$N_{\pm} = N\,\frac{e^{\pm \mu B/kT}}{e^{\mu B/kT} + e^{-\mu B/kT}} \approx \frac{1}{2}N\left(1 \pm \mu B/kT\right) \qquad [4]$$

Calculating thermal polarization using [3] we get

$$P(T) = \frac{\mu B_0}{k_B T} = \frac{\gamma \hbar B_0}{2k_B T} \qquad [5]$$

Even at several Tesla this interaction energy μB_0 is tiny compared to body temperature thermal jostling energies $k_BT \approx 1/40$eV. Thus, we do not expect a big difference in the populations of the two spin states as is confirmed in **Table 1**

Nucleus	μ (μ_N)	f (MHz)	$P_{1.5}$	Max Enhance
^{1}H	2.79	63.8595	4.9×10^{-6}	2.0×10^{5}
^{3}He	2.13	48.6467	3.8×10^{-6}	2.7×10^{5}
^{13}C	0.70	16.0570	1.2×10^{-6}	8.1×10^{5}
^{15}N	0.28	6.4708	5.0×10^{-5}	2.0×10^{6}
^{129}Xe	0.77247	17.6639	1.4×10^{-6}	7.3×10^{5}

Table 1 Moments, frequencies, and polarizations calculated using B_0 =1.5T,T=37°C,μ_N=5.05×10^{-27}J/T, h=6.623×10^{-34}J-s, k_B=1.38×10^{-23}J/K.

3. RELAXATION

Hyperpolarization is a battle to inject artificial levels of order into the spin system before nature returns things back to disorderly equilibrium. Thus, before we can understand about polarizing nuclei we need to understand a bit about how they relax.

A simple, intuitive (and relatively accurate) way of thinking about relaxation follows. A nuclear moment is continually being exposed to magnetic perturbations H_{pert} which persist for some correlation time τ_c. These perturbations can be caused by neighboring magnetic moments, and their variability stems from on-going collisions, vibrations and rotations. Just as application of an rf pulse causes a spin to rotate away from the z-axis, we can think of each H_{pert} event causing an infinitesimal rotation

$$\theta_{pert} = \gamma H_{pert} \tau_c \qquad [6]$$

Since these perturbations are randomly oriented, the cumulative angle of the spin will also follow a random walk. Collisions of duration τ_c will occur at a rate of R_c and thus after a time T_1 the total number of perturbations will have pushed the mean square angular rotation of the spin to something resembling "relaxed" $(\pi/2)^2$ which we will just take as unity since we're approximating anyway.

$$\theta_{tot}^2 \approx \left\langle \theta_{pert} \right\rangle^2 T_1 R_c \approx 1 \qquad [7]$$

$$\frac{1}{T_1} \approx R_c \left(\gamma H_{pert} \tau_c \right)^2 \qquad [8]$$

For nuclei in molecules, $R_c=1/\tau_c$, thus simplifying the relaxation rate to $1/T_1 \approx (\gamma H_{pert})^2 \tau_c$ which is often seen in the literature. This rough estimate is valid when the frequencies of the motions are much faster than the Larmor frequency of the spins $1/\tau_c >> \omega_0$. such as for gas atoms or small molecules. A proper treatment of relaxation can be found one of our favorite NMR texts such as Abragam [2].

3.1 Relaxation Time Estimates

Using the above equation, we can gain a good sense of the sorts of relaxation times we expect for various nuclei we might polarize.

^{3}He - During a collision, the perturbing field experienced by one ^{3}He atom due to the nuclear moment of the other is $H_{pert} \approx \mu_{3He}/r^3 \approx 1$G. The collision duration is roughly $\tau_c \approx r/v \approx 1$ps and the collision rate $R_c = [^3\text{He}]\sigma v \approx 1\times10^4 \text{s}^{-1}$. Using these numbers, we predict a gas phase relaxation time of about 640hr at 1atm which is close to the proper answer of T_1=750hr [3]. If we substitute paramagnetic oxygen with a 1000 fold higher magnetic moment we get a relaxation time of only $T_1 \approx 2.3$s which is again close to the real answer [4]. Relaxation times of 10's to 100's of hours are routinely observed for ^{3}He in high-purity containers, but only 10's of seconds are seen *in vivo*.

^{129}Xe – Like ^{3}He, ^{129}Xe experiences long relaxation times on the order of hours. Dipole-dipole relaxation is staggeringly long given the small magnetic moment of ^{129}Xe. However, ^{129}Xe relaxation is dominated by the spin rotation interaction which can be thought of as imperfect following of the large Xe electron cloud around its nucleus during a collision, causing a fluctuating magnetic field. The perturbing field from the spin rotation interaction in Xe-Xe collisions is roughly H_{SR}=0.7G. Xenon collisions involve molecule formation which at 1atm yields lifetimes are around 0.3ns, a correlation time 3 orders of magntitude longer than in binary ^{3}He-^{3}He collisions. The Xe molecular formation rate at 1atm is about $4\times10^7 \text{s}^{-1}$, gives us an estimated T_1 for gaseous ^{129}Xe around 3hrs which is about what is observed [5]. Solid phase ^{129}Xe relaxation can be very long, 2.4hrs at 77K and 100's of hours at 4.2K [6].

^{13}C –^{13}C relaxation times are much much shorter than for the noble gases. For a ^{13}C atom that is a typical 1.06 Angstrom bond length from a ^{1}H atom, the perturbing dipolar field will be $H_{pert} = \hbar\gamma/2r^3 \approx 14$G. Motional correlation time can be estimated from the rotating rigid dumbbell approximation with $A\omega = \hbar L$, where A is its moment of intertia and L is its angular momentum. The correlation time for rotation is then

$\tau_c \approx \pi m^* R^2/\hbar$. For a small molecule $\tau_c \approx 10^{-10}$s, leading us to predict a T_1 of about 40s. In real molecules a ^{13}C atom will have numerous neighboring ^{1}H atoms contributing to relaxation, further reducing that number. For medium size molecules (C_{10}-C_{50}), T_1 values ranging from 0.1s to 20s are observed. For very small molecules, highly symmetric molecules relaxation times exceeding 100s are possible. A good reference for ^{13}C relaxation is Breitmaier [7].

^{15}N – The smaller magnetic moment of ^{15}N results in ~6-fold longer relaxation times than ^{13}C.

^{1}H –The magnetic moment for ^{1}H is 4× larger than ^{13}C, leading to ~16× faster relaxation.

Nucleus	H_{pert} (G)	τ_c (s)	R_c (s^{-1})	T_1(max)
^{3}He	1	10^{-12}	10^4	750hr
^{129}Xe	1	10^{-9}	10^7	3hr
^{15}N	1-14	10^{-10}	10^{10}	10 min
^{13}C	1-14	10^{-10}	10^{10}	100s
^{1}H	1-20	10^{-10}	10^{10}	3s

Table 2 Relaxation estimates for polarized nuclei

4. THERMAL POLARIZATION METHODS

Very roughly one can classify the various methods of hyperpolarization into two categories - those based in thermal polarization and those based in optical polarization. The thermally-derived methods are known as *brute force polarization*, *parahydrogen-induced polarization*, and *dynamic nuclear polarization*.

4.1 Brute Force Polarization

Perhaps the most intuitive way of imparting polarization is to take thermal equilibrium to its extreme. Magnetic field strengths of 15T are becoming routine and temperatures in the 10mK regime are regularly achieved using ^{3}He dilution refrigerators. Below 100mK polarization is

$$P = \tanh\left(\frac{\mu B_0}{k_B T}\right) \qquad [9]$$

At 15T and 10mK, for example, we predict thermal polarization levels of 91%, 82%, 37%, 15%, and 40% for ^{1}H, ^{3}He, ^{13}C, ^{15}N, and ^{129}Xe respectively. Unfortunately, as one lowers temperature, the thermal motions which give rise to spin lattice relaxation start to "freeze out" and T_1 can become enormously long. Methods have been proposed to overcome this problem via the addition of a paramagnetic agents such as O_2 or even using liquid ^{3}He (whose motions do not freeze out) to relax the desired target nuclei distributed over high surface areas. Methods for ultra-low temperature polarization of ^{3}He involving a combination of liquid ^{3}He and solid ^{3}He have been proposed by Frosatti [8]. Kjurkov and co-workers have recently polarized ^{129}Xe at 15T and down to 15mK by brute force using liquid ^{3}He to shorten relaxation times of thin layers of ^{129}Xe distributed over a large surface area material [9].

4.2 Para-Hydrogen Induced Polarization – PHIP

Molecular hydrogen contains two protons which can combine as a singlet with anti-aligned nuclear spins or as a triplet state with aligned nuclear spins. Because protons are fermions, the wavefunction of the whole molecule must be antisymmetric under exchange of the protons. Since the parahydrogen nuclear spin state is antisymmetric it must adopt a symmetric rotational state (J=0,2,4…). Similarly, the ortho-hydrogen with its symmetric spin wave function, must adopt an antisymmetric rotational state (J=1,3,5…). Thus, the energy difference between the parahydrogen and orthohydrogen is set by the *rotational energy scales*, not the tiny nuclear magnetic energy scale. With an energy difference of 0.015eV between o-H_2 and p-H_2, only modest cryogenic temperatures (T<20K) are required to convert practically all the hydrogen to the para- form. An excellent and recent review of the thermodynamics of parahydrogen is given by Jonischkeit [10]. Note that parahydrogen is <u>not</u> polarized. It has no NMR signal of its own, but it has an extremely high degree of spin order which can be subsequently turned into polarization through suitable trickery.

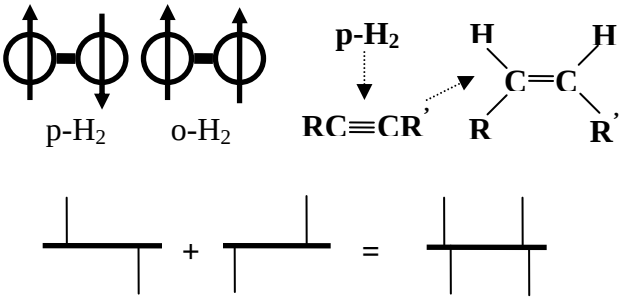

Figure 1 A. Para vs ortho-hydrogen. **B.** Schematic hydrogenation reaction. **C.** Parahydrogen spectra from isolated molecules add to give the observed spectrum Small frequency shifts due to j-coupling prevent total cancellation of magnetization

If the parahydrogen molecule can be transferred in its entirety to a suitable substrate molecule via a chemical reaction that is fast compared to the relaxation of the transferred ^{1}H atoms (a few seconds), and the new locations of those ^{1}H atoms are somehow distinguishable from one another (through chemical shifts), then large anti-phase magnetization should be observable as shown in **Figure 1**. On any given molecule, one hydrogen gives an emission spectrum while the other yields an absorption spectrum. Since p-H_2 reacts in random orientations on the substrate, this would seem to cancel out all the magnetization. However, j-couplings cause a spin up hydrogen atom to shift the frequency of its spin-down neighbor differently than a spin-down hydrogen shifts a spin-up. Thus, total anti-phase signal is preserved as shown in the diagram. This method was named the PASADENA effect by its discovers Bowers and Weitekamp in 1986 [11].

A breakthrough for imaging came when Axelsson and co-workers realized that one further step could be implemented to translate this anti-phase ^{1}H magnetization in to real ^{13}C magnetization. [12]. By lowering the magnetic field non-adiabatically to a very low value, the spin state evolution is dominated by the tiny electron mediated j-couplings. By allowing all the coupled spins to evolve for about 1sec in this ultra low-field, the anti-phase ^{1}H magnetization can be trapped in the ^{13}C atoms. The field is then adiabatically ramped back up, locking in the ^{13}C polarization as discussed by Goldman [13].

4.3 Dynamic Nuclear Polarization – DNP

Dynamic Nuclear Polarization uses the much larger interaction energy of an electron spin with the magnetic field to create high nuclear polarizations at more moderate temperatures and magnetic fields. An electron possesses a magnetic moment that is 657-fold larger than the moment of a proton, and thus at only 1.2K and a magnetic field of 3T, the electronic spin polarization will be 95%. Off-resonance microwave radiation can impart "electron-like" polarization levels to the nuclei of interest.

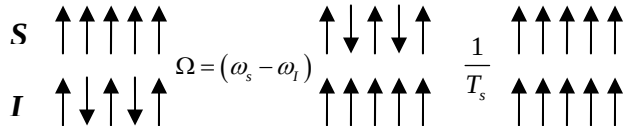

Figure 2 Schematic representation of the DNP process.

To understand DNP conceptually, we consider an assembly of nuclear spins *I* embedded in a solid that contains a few paramagnetic impurities of spin *S*. Neighboring nuclear and electron spins share a contact hyperfine interaction of form $I \cdot S$ which allows electron-nuclear flip-flop transitions. As shown in **Figure 2,** initially all the electron spins *S* are up (polarized), while the nuclear spins *I* are randomly mixed between up and down (un-polarized). We now apply microwave radiation at a frequency $\Omega = (\omega_s - \omega_I)$ which drives electron-nuclear flip-flops. Since all electron spins are initially pointed up, nuclear spins pointed up cannot be flipped because that's not a flip-flop, so those nuclei stay up. Nuclear spins initially pointed down, however, *can* flip up while a neighboring electron spin flips down. Once it has flipped down, the electron spin is very rapidly returned to the up position by spin-lattice relaxation T_s^{-1}. Thus, we have a one-way street creating high nuclear spin polarization. Similarly, one could show that applying off-resonance radiation at $\Omega = (\omega_s + \omega_I)$ would cause flip-flip transitions and create a negative nuclear polarization.

Several constraints are necessary for effective DNP. First, we have assumed that when we apply flip-flop radiation, we induce no flip-flips. This is equivalent to requiring a narrow line-width for the free-electron ESR line. Second, we have just established that the electron spins need to relax quickly after they have flipped down. Similarly, the nuclear spins must not relax by other means compared to the timescale it takes to get them all aligned by DNP. Under carefully tailored circumstances this can be achieved. A good review of DNP is given by Abragam and Goldman [14].

In their pioneering work, Ardenkjaar-Larsen and co-workers describe in detail the method they use to polarize ^{13}C labeled Urea and extract it for *in vivo* imaging [15]. Urea (8.27mmol) is dissolved in a glycerol-water mixture and a trityl radical is added to supply the free electrons. This mixture is frozen into pellets in liquid nitrogen and lowered into the bore of the cryostat which is running at 3.35T and 1.2K. At that field strength, the electron-nuclear flip-flop transition is driven with 94GHz microwave radiation with a power of 200mW. ^{13}C polarization builds up with a time constant of about 1.4hr. After sufficient build-up, the frozen sample is raised out of the liquid helium bath, 7ml of boiling water is injected in and the dissolved hyperpolarized mixture is ejected into a second container. The sample must be imaged within seconds before the ^{13}C magnetization decays away. DNP is potentially the most versatile hyperpolarization technique and could be used to polarize any nucleus.

5. OPTICAL HYPERPOLARIZATION

The optical methods use angular momentum transfer to create polarization. From the perspective of optical polarization, the difference between spins $\uparrow\downarrow$ and $\uparrow\uparrow$ is one quantum of angular momentum $\hbar$, which is conveniently what a photon carries. If we can just inject the necessary angular momentum into an un-polarized ensemble of spins, it becomes polarized. The two optical methods which use this principle to polarize the noble gas isotopes are *spin exchange optical pumping* and *metastability exchange optical pumping* which have become affectionately known as SEOP and MEOP. The first step of polarization is optical pumping which creates high *electron* spin polarization at room temperature. The next step in the process is some sort of collisional transfer of electron polarization to nuclear polarization.

Optical pumping relies on the fact that both energy and angular momentum must be conserved when an atom absorbs a photon. Consider the hypothetical atom in **Figure 3** with a ground state and an excited state that have no orbital angular momentum, only electron spin S=1/2. Of course, energy is conserved by tuning a laser to the appropriate wavelength of the optical transition. But if we are shining in circularly polarized light (denoted σ+ and σ- for right and left handed), each photon carries $\pm 1\hbar$ of angular momentum, and this also must be conserved. Angular momentum conservation then dictates that only atoms whose ground state spin is initially down can absorb an incoming σ+ photon. Those with spin up, have no allowed transition to the excited state because there's no angular-momentum-conserving 3/2 excited state to jump to. Eventually, all the spin down atoms are pumped out and once they land in the spin up ground state, they're "in the dark". This process then leads to highly polarized electron spins. The next step is to translate that electron polarization to nuclear polarization which in both methods happens via collisions.

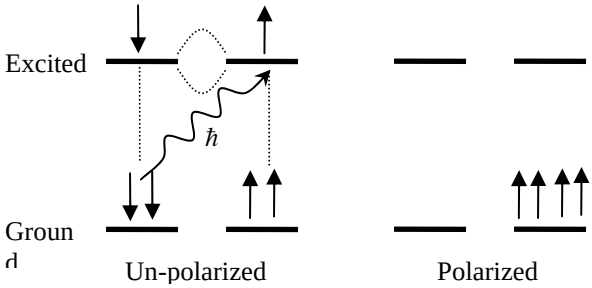

Figure 3 Schematic of the optical pumping process

5.1 Spin Exchange Optical Pumping – SEOP

Optical pumping and spin exchange is applicable to polarizing ^{3}He or ^{129}Xe. For this method, the hypothetical atom is an alkali metal atom, usually Rb whose 795nm D_1 transition is readily accessible to high-power diode laser arrays. Typically a blob of Rb resides on the bottom of a glass chamber which is filled with the noble gas to be polarized as well as some other buffer gases. The chamber is heated to create a dilute Rb vapor so that it can absorb resonant circularly polarized light from a laser. Optical pumping creates a high electron spin polarization in the Rb vapor, somewhat analogous to DNP, except at high temperature and in the gas phase.

Transfer of the polarization from electron spins to nuclear spin again happens by the $I \cdot S$ hyperfine interaction. This interaction only occurs during the very brief collisions between the alkali and noble gas atoms allowing an electron spin to flip from up to down, while the nuclear spin flips from down to up. The alkali metal then goes off and absorbs another photon to regain its polarization. Because spin exchange occurs during collisions the energy difference of the electron-nuclear spin flip-flop can be supplied or carried away by the momentum of the colliding atoms. Thus, unlike DNP, no additional radiation needs to be supplied. However, just like

DNP, the noble gas relaxation by other mechanisms must be slow compared to the spin exchange.

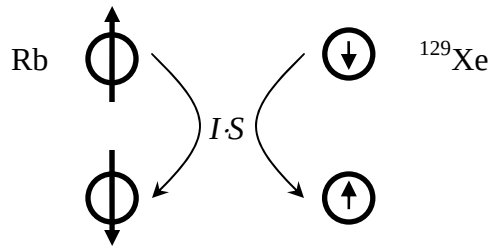

Figure 4 Spin exchange collisions between Rb and ^{129}Xe

^{3}He SEOP - In a typical ^{3}He polarizer, a 150cm^{3} high-purity glass sphere is filled with 10atm of ^{3}He 0.01atm N_2 for fluorescence quenching, giving about 1.3 liters of "dispensable" ^{3}He. The "cell" is heated to about 180°C to create an alkali metal vapor density of about 10^{-5}atm to absorb the laser light. Circularly polarized laser light at a power of 50W or so provides the optical pumping. The polarization build-up occurs with a time constant of about 4-5hrs. Typical polarization levels are 25-50%, with values as high as 74% having been observed [16]. A good overview of ^{3}He polarization is given by Leawoods [17].

^{129}Xe SEOP – ^{129}Xe polarization uses the exact same physics just described. However, due to the high nuclear charge of ^{129}Xe, its interaction with the alkali valence electron is so potent that the alkali cannot maintain its polarization unless the ^{129}Xe is quite dilute. Thus, in a typical system, a partial pressure of only 0.05atm of Xe is combined with 5-10atm of ^{4}He buffer gas to broaden the Rb absorption line to absorb as much light as possible. With laser power levels of 50W or so, the ^{129}Xe polarization builds up with a time scale of 10-20sec in the optical pumping cell. The gas mixture flows continuously such that a given Xe atom spends 30sec or so in contact with the optically pumped alkali metal atoms before exiting the optical cell highly polarized. ^{129}Xe is separated from the ^{4}He buffer gas at 77K where Xe forms an ice cube with T_1 of about 2.4hrs, while the ^{4}He is vented into the air. Once a sufficient ice cube has been accumulated, it is thawed rapidly and collected in a dose delivery bag [6]. Typical polarizers produce about 0.5liters per hour with a polarization on order 10%. Recently great advancements in polarization (>40%) and production rate (5 liters/hr) have been reported [18].

5.2 Metastability Exchange Optical Pumping

Under suitable conditions, direct optical pumping of ^{3}He is possible, resulting in highly efficient conversion of polarized light into polarized nuclei. The ground state of ^{3}He is not suitable for optical pumping because it has no net spin (both electrons are in the 1s ground state). However, by running a weak rf discharge at low ^{3}He pressures (1-3 Torr) a small fraction of the ^{3}He atoms (~10^{-7}) are promoted to a metastable state denoted ^{3}He* where the electron configuration is now 1s2s. The electron in the 2s state now looks for all intents and purposes like the valence electron of an alkali metal and can be optically pumped using circularly polarized 1083nm light. As with alkali metal optical pumping, the continuous absorption of angular momentum from circularly polarized light leads to depletion of the spin down 2s state and high electronic polarization. Hyperfine coupling $I \cdot S$ between the ^{3}He nuclear spin I and the now polarized 2s electron spin S yields equally high nuclear polarization on the same ^{3}He* atom. The process is completed through a metastability exchange collision wherein a polarized metastable ^{3}He* collides with an unpolarized stable ^{3}He atom and transfers its metastability while retaining its high nuclear polarization. The newly metastable ^{3}He* atom is now ready for optical pumping.

The power of this method is that it is incredibly efficient with photons. Nearly each absorbed photon is translated into a nuclear spin and therefore nuclear polarization build-up happens on a timescale of seconds. However, the process necessarily has to be conducted at very low pressures in order to 1) maintain the RF discharge 2) maintain a sufficient lifetime of the ^{3}He* atoms 3) retain the hyperfine structure of the ^{3}He* atoms for optical pumping. This introduces two difficulties 1) the need to compress the gas to atmospheric pressure after polarization and 2) the need to use a very narrow-band laser source at 1083nm to perform the optical pumping on the right hyperfine transition.

The state-of-the art MEOP system including 4 1 meter long optical pumping cells, 2 15W narrow-band LNA lasers, and all the compression has been pioneered by professors Ernst Otten and Werner Heil at Mainz university. **Figure 5** shows a schematic of the metastable system with a benchmark performance of a stunning 5liters/hr at P=50% with polarization levels rising beyond 70% for reduced flows. These systems of which there are 1 or 2 in the world are truly a sight to behold. Metastability exchange polarization

works only for ^{3}He and not for ^{129}Xe because metastable Xe* is in a p orbital and quickly loses its spin angular momentum to its orbital angular momentum.

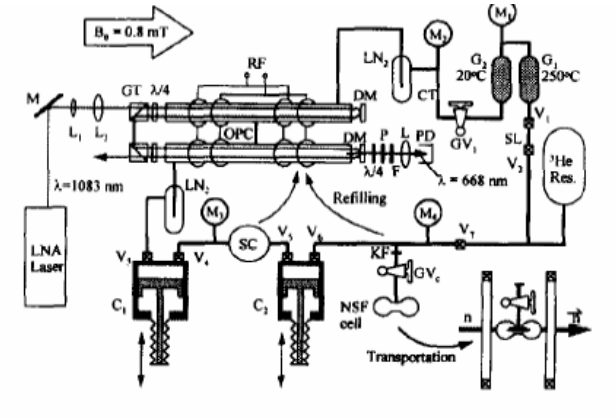

Figure 5 Schematic of the Mainz metastable 3He Polarization System

A complete review of a MEOP polarization is given by Surkau [19], while a nice introductory overview is given by Otten [20]. An excellent resource for the latest status of MEOP technology as well as all manner of hyperpolarization is the on-line 2002 Helion conference proceedings [21].

6. CONCLUSIONS

Generally speaking, hyperpolarized substances make it possible to detect things that weren't previously detectable. Gases can be imaged with tissue-like resolution and ^{13}C angiography is possible with extraordinary speeds and no background signal. The potential exists for all agents to make equally good images at low magnetic field as at high field because the magnetization is not created by the imaging magnet. We have yet to see the full exploitation of chemical shift sensitivity, particularly for ^{129}Xe, ^{13}C and ^{15}N. A good review of clinical hyperpolarized ^{3}He MRI has been given by Salerno *et al.*,., [22]. A very thorough review of ^{129}Xe MRI was recently published by Oros and Shah [23]. A good review of the potential of ^{13}C can be found in Golman [24]. The best, ideas are yet to come especially when these exciting technologies become better disseminated.

In closing, it is worthwhile to briefly summarize the current technical specifications and status of the various methods. ^{3}He imaging is probably most disseminated and numerous groups are actively imaging patients and volunteers. ^{129}Xe imaging is starting to emerge with a handful of groups performing human work. As of this writing ^{13}C in vivo imaging using both DNP and PHIP has been limited to small animals and just 1 group with another handful performing *in vitro* studies. Finally, brute force polarization is largely a theoretical idea with a handful of groups performing proof of concept studies. The table below summarizes current technical performance benchmarks.

Method	Nuclei	P_{max} (%)	mmol/hr
Brute Force	All	41	10
PHIP	^{1}H, ^{13}C, ^{15}N	20	300
DNP	^{13}C, ^{15}N	40	6
^{3}He SEOP	^{3}He	74	13
^{129}Xe SEOP	^{129}Xe	40	200
^{3}He MEOP	^{3}He	70	200

Table 3 Simplified comparison of the hyperpolarization methods and current performance capabilities.

7. REFERENCES

[1] M. S. Albert, G. D. Cates, B. Driehuys, W. Happer, B. Saam, C. S. Springer, and A. Wishnia, "Biological Magnetic-Resonance Imaging Using Laser Polarized ^{129}Xe," *Nature*, vol. 370, pp. 199-201, 1994.

[2] A. Abragam, *Principles of Nuclear Magnetism*. New York: Oxford University Press, 1961.

[3] N. R. Newbury, A. S. Barton, G. D. Cates, W. Happer, and H. Middleton, "Gaseous He-3 He-3 Magnetic Dipolar Spin Relaxation," *Physical Review A*, vol. 48, pp. 4411-4420, 1993.

[4] B. Saam, W. Happer, and H. Middleton, "Nuclear relaxation of ^{3}He in the presence of O_2," *Phys. Rev. A*, vol. 52, pp. 862-865, 1995.

[5] B. Chann, I. A. Nelson, L. W. Anderson, B. Driehuys, and T. G. Walker, "^{129}Xe-Xe molecular spin relaxation," *Physical Review Letters*, vol. 88, pp. 113201, 2002.

[6] B. Driehuys, G. D. Cates, E. Miron, K. Sauer, D. K. Walter, and W. Happer, "High-volume production of laser-polarized Xe-129," *Applied Physics Letters*, vol. 69, pp. 1668-1670, 1996.

[7] E. Breitmaier, K. Spohn, and S. Berger, "13C Spin-Lattice Relaxation Times and Mobility of Organic Molecules in Solution," *Angew. Chem. Int. Ed.*, vol. 14, pp. 144-159, 1975.

[8] G. Frossati, "Polarization of ^{3}He, D_2 (and possibly ^{129}Xe) using cryogenic techniques," *Nuclear Instruments & Methods in Physics Research A* -

Accelerators Spectrometers Detectors and Associated Equipment, vol. 402, pp. 479-483, 1998.

[9] E. V. Krjukov, J. D. O'Neill, and J. R. Owers-Bradley, "Brute force polarization of Xe-129," *Journal Of Low Temperature Physics*, vol. 140, pp. 397-408, 2005.

[10] T. Jonischkeit and K. Woelk, "Hydrogen Induced Polarization-Nuclear-Spin Hyperpolarization in Catalytic Hydrogenations without the Enrichment of Para- or Orthohydrogen," *Adv. Synth. Catal.*, vol. 346, pp. 960-969, 2004.

[11] C. R. Bowers and D. P. Weitekamp, "Transformation of Symmetrization Order to Nuclear-Spin Magnetization by Chemical Reaction and Nuclear Magnetic Resonance," *Physical Review Letters*, vol. 57, pp. 2645-2648, 1986.

[12] K. Golman, O. Axelsson, H. Johannesson, S. Mansson, C. Olofsson, and J. S. Petersson, "Parahydrogen-induced polarization in imaging: Subsecond ^{13}C angiography," *Magnetic Resonance in Medicine*, vol. 46, pp. 1-5, 2001.

[13] M. Goldman, H. Johannesson, O. Axelsson, and M. Karlsson, "Hyperpolarization of C-13 through order transfer from parahydrogen: A new contrast agent for MRI," *Magnetic Resonance Imaging*, vol. 23, pp. 153-157, 2005.

[14] A. Abragam and M. Goldman, "Principles of Dynamic Nuclear Polarization," *Reports on Progress in Physics*, vol. 41, pp. 395-467, 1978.

[15] J. H. Ardenkjaer-Larsen, B. Fridlund, A. Gram, G. Hansson, L. Hansson, M. H. Lerche, R. Servin, M. Thaning, and K. Golman, "Increase in signal-to-noise ratio of >10,000 times in liquid-state NMR," *Proc. Nat. Acad. Sci.*, vol. 100, pp. 10158-10163, 2003.

[16] E. Babcock, I. Nelson, S. Kadlecek, B. Driehuys, L. W. Anderson, F. W. Hersman, and T. G. Walker, "Hybrid spin-exchange optical pumping of He-3," *Physical Review Letters*, vol. 91, 2003.

[17] J. C. Leawoods, "Hyperpolarized 3He Gas Production and MR Imaging of the Lung," *Concepts in Magnetic Resonance*, vol. 13, pp. 277-293, 2001.

[18] I. C. Ruset, S. Ketel, and F. W. Hersman, "Large Volume Production and Delivery of Hyperpolarized 129Xe," presented at Proc. Intl. Soc. Mag. Reson. Med. 13, Miami, 2005.

[19] R. Surkau, J. Becker, M. Ebert, T. Grossman, W. Heil, D. Hofmann, H. Humblot, M. Leduc, E. W. Otten, D. Rohe, K. Siemensmeyer, M. Steiner, F. Tasset, and N. Trautmann, "Realization of a Broad Band Neutron Spin Filter with Compressed, Polarized 3He Gas," *Nucl. Instr. and Meth. in Phys. Res. A*, vol. 384, pp. 444-450, 1997.

[20] E. Otten, "Take a breath of polarized noble gas," *Europhysics News*, vol. 35, 2004.

[21] Helion02, in *International Workshop on Polarized 3He Beams and Gas Targets and Their Applications*. Oppenheim, Germany, 2002, pp. http://www.physik.uni-mainz.de/helion02/.

[22] M. Salerno, T. A. Altes, J. P. Mugler, M. Nakatsu, H. Hatabu, and E. E. DeLange, "Hyperpolarized Noble Gas MR Imaging of the Lung: Potential Clinical Applications," *Eur. J. Radiology*, vol. 40, pp. 33-44, 2001.

[23] A. Oros and N. J. Shah, "Hyperpolarized xenon in NMR and MRI," *Phys. Med. Biol.*, vol. 49, pp. R105-R153, 2004.

[24] K. Golman, J. H. Ardenkjaer-Larsen, J. S. Petersson, S. Mansson, and I. Leunbach, "Molecular Imaging with Endogenous Substances," *Proc. Nat. Acad. Sci.*, vol. 100, pp. 10435-10439, 2003.